PHILOSOPHICAL TRANSACTIONS OF THE ROYAL SOCIETY A MATHEMATICAL, PHYSICAL & ENGINEERING SCIENCES

# Analysis of the Flexural Vibrations of Variable Density Spheroids Immersed in an Ideal Fluid, with Application to Ship Structural Dynamics

R. Eatock Taylor

*Phil. Trans. R. Soc. Lond. A* 1975 **277**, 623-646
doi: 10.1098/rsta.1975.0017

# ANALYSIS OF THE FLEXURAL VIBRATIONS OF VARIABLE DENSITY SPHEROIDS IMMERSED IN AN IDEAL FLUID, WITH APPLICATION TO SHIP STRUCTURAL DYNAMICS

By R. EATOCK TAYLOR
*Department of Mechanical Engineering, University College London, Torrington Place, London WC1E 7JE*

(*Communicated by Sir William Hawthorne, F.R.S. – Received* 24 *January* 1974)

## CONTENTS



An analysis is given of the characteristic flexural modes and frequencies of a linearly elastic free–free spheroid in an ideal fluid. The finite element method is used to represent the structural properties of a slender spheroid, employing a special element formulated for this purpose on the basis of Euler–Bernoulli beam theory. A consistent added mass matrix is derived from the exact solution of the infinite fluid potential problem, truncated at a suitable number of terms. A consistent added stiffness matrix is obtained for the buoyancy forces on a spheroid floating with its axis in a free surface, but other free surface effects (associated with wave generation) are assumed negligible. Solutions are computed for different aspect-ratio variable density spheroids *in vacuo*, deeply submerged, and floating. The results indicate the possibility of considerable distortions in the lowest ('rigid') modes of slender floating bodies vibrating in a vertical plane, and illustrate the difficulty of defining three dimensional reduction factors for use with a simplified two dimensional theory. Derivation of the classical reduction factors for uniform density spheroids is given by way of comparison. The paper provides an illustration of use of a finite element formulation, in conjunction with consistent added mass and stiffness matrices, for a rational analysis of the structural dynamics of ships and other marine vehicles.

Vol. 277. A. 1274. 65 [Published 13 February 1975

## 1. Introduction

The research reported here is intended as a stage in the development of numerical methods for calculating ship structural response, leading to rational methods of evaluating the strength of ships in waves and of assessing response to propeller and engine-induced excitation. Structural dynamic problems are assuming a role of paramount importance with the increasing size and complexity of current ships. Analysis of these problems is difficult, involving mathematical representation and numerical evaluation of complex interactions, both structural and hydrodynamic. These include interaction between main hull and local response, and the three dimensional hydrodynamic problem.

Numerical methods of solving these problems are currently under development, and the finite element method is well advanced for idealization of the three dimensional structural properties of ships (Kendrick 1970; Hylarides 1971). Not so well established, however, are compatible methods of representing hydrodynamic interaction effects associated with vibrating ships. To assist in the development of these ideas, it was proposed first to consider simple configurations and to use the results from such studies to evaluate numerical methods for more realistic cases. From the vibration standpoint, the simplest relevant configuration is the uniform beam; study of this has led to valuable insight into the response of ships to dynamic loads, particularly wave-induced response (Bishop & Eatock Taylor 1973). From the point of view of three dimensional hydrodynamic calculations, the spheroid is one of the most straightforward geometries. For this reason flexural vibrations of a spheroid are analysed in this paper.

Certain results for spheroids have in fact long been used in ship structural dynamic calculations. This is because, in the analysis of the structural dynamics of a ship as a free–free beam, it has been common practice to employ strip theory. This accounts for energy transfer between a vibrating ship and surrounding water by first assuming the flow past hull cross-sections to be two dimensional, hence obtaining an added mass corresponding to the section. The added mass of every section is then modified by a reduction factor to take account of the three dimensionality of the flow. The factor $J_r$ is associated with an assumed $r$th vibration mode, and it is based on the three dimensional flow around a vibrating spheroid of the same length/breadth ratio as the ship. This paper presents a modal analysis for prolate spheroids and describes the relation between $J_r$ and the mode shape.

Clearly the modes depend upon the degree of material non-uniformity of the spheroid. Previous investigations (see, for example, Lewis 1929; Lockwood Taylor 1930; Kruppa 1962; Landweber 1971) have given results for mode shapes approximating the behaviour of spheroids only of uniform density and elasticity, and have neglected the influence of added stiffness due to buoyancy effects on floating bodies. The latter might lead to significant distortion in the lowest modes in the vertical plane (conventionally termed heave and pitch) of relatively flexible ships such as Great Lakers; but the phenomenon appears to have been disregarded until recently (Bishop 1971; Bishop, Eatock Taylor & Jackson 1973).

Uniform and non-uniform spheroids, floating and submerged, are analysed here by the finite element method, and results are compared with those from previous analyses re-derived in the first part of this paper. Finite element mass and stiffness matrices are developed for a spheroidal element. A consistent added mass matrix for this element is derived from the exact fluid potential theory, and a consistent added stiffness matrix is obtained for buoyancy forces. The results illustrate use of these matrices to obtain mode shapes, frequencies and reduction factors $J_r$ for spheroids.



PHILOSOPHICAL TRANSACTIONS OF THE ROYAL SOCIETY A MATHEMATICAL, PHYSICAL & ENGINEERING SCIENCES

### 1.1. *Notation*

| | |
|---|---|
| $a$ | major semi-axis of ellipse |
| $a_p, c_p$ | coefficients in series expansions |
| $A$ | finite element sectional area |
| $b$ | minor semi-axis of ellipse |
| $\boldsymbol{D}$ | matrix given by (20) |
| $\boldsymbol{D}_0$ | matrix given by (38) |
| $\bar{\boldsymbol{D}}$ | matrix given by (25) |
| $E$ | Young modulus |
| $\boldsymbol{E}$ | inverse of $\boldsymbol{D}$ |
| $\bar{\boldsymbol{E}}$ | inverse of $\bar{\boldsymbol{D}}$ |
| $g$ | acceleration due to gravity |
| $I$ | finite element sectional moment of inertia |
| $J_r$ | three dimensional correction factor for $r$th mode |
| $\boldsymbol{k}$ | added stiffness matrix |
| $\boldsymbol{K}$ | stiffness matrix |
| $l$ | finite element length |
| $\boldsymbol{m}$ | added mass matrix |
| $\bar{\boldsymbol{m}}$ | transformed added mass matrix |
| $\boldsymbol{M}$ | mass matrix |
| $\boldsymbol{n}$ | outward normal to surface of spheroid |
| $N$ | number of elements in finite element idealization |
| $p, r, s$ | indices |
| $P$ | number of terms in hydrodynamic solution |
| $P_r$ | Legendre polynomial of degree $r$ |
| $\boldsymbol{q}$ | vector of generalized coordinates |
| $\boldsymbol{q}^*$ | transformed vector of generalized coordinates |
| $\boldsymbol{q}_0$ | vector of finite element nodal displacements |
| $\boldsymbol{R}$ | diagonal matrix given by (27) |
| $t$ | element number, time |
| $T$ | kinetic energy of element |
| $T_{\mathrm{f}}$ | fluid kinetic energy |
| $\bar{T}_{\mathrm{f}}$ | fluid kinetic energy in two dimensional motion |
| $T_p^m$ | associated Legendre function of the first kind of degree $p$ |
| $u$ | longitudinal displacement of point on surface of spheroid |
| $U_p^m$ | associated Legendre function of the second kind of degree $p$ |
| $V$ | elastic strain energy of element |
| $w$ | transverse displacement of point on surface of spheroid |
| $x, y, z$ | Cartesian coordinates |
| $\boldsymbol{X}$ | vector of influence functions given in appendix B |
| $\eta, \chi$ | dimensionless coordinates at ends of spheroidal element |
| $\kappa$ | parameter for ellipse $(= (a^2 - b^2)^{\frac{1}{2}})$ |
| $\mu, \theta, \nu$ | spheroidal coordinates |
| $\nu_0$ | value of $\nu$ on surface $S$ of spheroid |
| $\xi$ | non-dimensional coordinate $(= x/l)$ |
| $\rho_{\mathrm{b}}$ | body density |
| $\rho_{\mathrm{f}}$ | fluid density |
| $\sigma_1, \sigma_2, \tau_1, \tau_2, \tau_3, \tau_4$ | functions of $\eta$, $\chi$ given in appendix B |
| $\phi$ | velocity potential |
| $\omega$ | frequency of vibration |
| $\omega_r$ | $r$th natural frequency |

*dressings*

| | |
|---|---|
| $'$ | transpose of a matrix |
| $t$ | superscript denoting element property |

## 2. Solutions for three dimensional ideal flow around oscillating spheroids

### 2.1. *Some general results*

Throughout this paper it is assumed that the flow is incompressible and inviscid. Evidence published to date suggests that this is a realistic assumption for vibrations of ships in the vertical plane, and it is a good starting point for analysis of coupled horizontal-torsional vibrations.

A velocity potential $\phi$ may then be used, satisfying the Laplace equation

$$\nabla^2\phi = 0 \tag{1}$$

throughout the fluid region (assumed infinite at this stage), and a Neumann boundary condition on the surface $S$ of the spheroid. The flow is assumed to result solely from the oscillatory motions of the spheroid, since this paper is concerned only with a body having zero forward velocity.†

A curvilinear coordinate system $(\mu, \theta, \nu)$ is employed, which is related to the Cartesian system $(x, y, z)$ by

$$\left.\begin{aligned} x &= \kappa\mu\nu \\ y &= \kappa(1-\mu^2)^{\frac{1}{2}}(\nu^2-1)^{\frac{1}{2}}\sin\theta \\ z &= \kappa(1-\mu^2)^{\frac{1}{2}}(\nu^2-1)^{\frac{1}{2}}\cos\theta, \end{aligned}\right\} \tag{2}$$

where

$$\kappa^2 = a^2 - b^2.$$

$a$ and $b$ are the major and minor semi-axes of the generating ellipse, and the spheroid is given by rotating this ellipse

$$x^2/a^2 + y^2/b^2 = 1, \quad a > b \tag{3}$$

about the $x$-axis. The surface $S$ of the spheroid is given by $\nu = \nu_0$ and the unit outward normal is $\boldsymbol{n}$.

Expressed in this system, the boundary condition on $\phi$ is

$$\partial\phi/\partial n = [\mu\dot{u} + (a/b)(1-\mu^2)^{\frac{1}{2}}\cos\theta\dot{w}](\nu_0^2-1)^{\frac{1}{2}}/(\nu_0^2-\mu^2)^{\frac{1}{2}} \quad \text{on} \quad S, \tag{4}$$

where $\dot{u}$ and $\dot{w}$ are longitudinal and transverse components of the surface velocity. The appropriate solution to Laplace's equation for a deeply submerged spheroid undergoing lateral vibrations of frequency $\omega$ is

$$\phi = \sum_{p=1}^{\infty} c_p T_p^1(\mu) U_p^1(\nu)\cos\theta\sin\omega t. \tag{5}$$

$T_p^1$ and $U_p^1$ are respectively associated Legendre functions of the first and second kind. Some properties of these functions are given in appendix A. The constants $c_p$ are obtained from the boundary condition by using the orthogonality of the functions $T_p^1$.

The kinetic energy $T_f$ of the ideal fluid of density $\rho_f$ surrounding the vibrating spheroid is given by

$$T_f = -\tfrac{1}{2}\rho_f\int_S \phi\frac{\partial\phi}{\partial n}\,\mathrm{d}S = -\frac{1}{2}\frac{\pi b^2\rho_f}{(a^2-b^2)^{\frac{1}{2}}}\sum_{p=1}^{\infty} c_p^2 U_p^1\frac{\mathrm{d}U_p^1}{\mathrm{d}\nu}\frac{2p(p+1)}{2p+1}\sin^2\omega t. \tag{6}$$

If however the harmonic motions of the spheroid are defined by a vector of generalized coordinates $\boldsymbol{q}$, the fluid kinetic energy may be written (Milne-Thomson 1968)

$$T_f = \tfrac{1}{2}\dot{\boldsymbol{q}}'\boldsymbol{m}\dot{\boldsymbol{q}}. \tag{7}$$

This equation defines an added mass matrix $\boldsymbol{m}$ corresponding to the generalized coordinates $\boldsymbol{q}$. The vector $\boldsymbol{q}$ is determined by the longitudinal and transverse components of the surface displacement, $u$ and $w$ respectively. For any particular motion the corresponding added mass matrix may therefore be found. Furthermore, a three dimensional added mass correction factor may be

† It should be noted that the influence of a ship's forward velocity on wave-induced vibration amplitudes is a problem to which a satisfactory solution has not yet been given. For a body in an infinite ideal fluid, hydrodynamic damping is thereby introduced, proportional to the forward velocity of the body. This is 'dynamic' (non-dissipative) damping. It corresponds to a transfer of energy between modes, analogous to the coupling introduced when vibrating systems are rotated.

obtained, if the two dimensional problem has been solved as well. For transverse motions of a slender body, this factor $J$ is defined by

$$J = \frac{\text{kinetic energy of fluid in three dimensional motion}}{\text{kinetic energy of fluid in two dimensional motion}}. \tag{8}$$

### 2.2. *The motions assumed by Lewis* (1929)

Consider first the simplest case, in which $u$ is taken as zero and $w$ as a function of $x$ only. This corresponds to all cross-sections translating laterally without rotation, and was the assumption made by Lewis (1929) in his study of the added masses of deforming spheroids. Kinematically this implies deformation of the body in pure shear. The displacement $w$ is written as a sum of a series of polynomials in the coordinate $\mu$, the coefficients $a_r$ of the series determining the shape of the deformed axis of the spheroid. Specifically

$$w(\mu) = \sum_{r=1}^{\infty} a_r \frac{T_r^1(\mu)}{(1-\mu^2)^{\frac{1}{2}}} \cos \omega t = \sum_{r=1}^{\infty} a_r \frac{\mathrm{d}P_r(\mu)}{\mathrm{d}\mu} \cos \omega t, \tag{9}$$

or

$$w(\mu) = \left[a_1(1) + a_2(3\mu) + a_3\left(\frac{15\mu^2-3}{2}\right) + \ldots\right] \cos \omega t.$$

The terms corresponding to $a_1$, $a_2$ and $a_3$ represent respectively heave, pitch and an approximate two node distortion of the spheroid. Calling these 'modes', in a somewhat loose terminology, we have thereby expressed $w$ as a sum of modes $w_r$

$$w(\mu) = \sum_{r=1}^{\infty} a_r w_r(\mu) \cos \omega t. \tag{10}$$

The coefficients $a_r \cos \omega t$ may, however, be thought of as generalized coordinates, so that we may let

$$\boldsymbol{q}' = [a_1 \cos \omega t \, a_2 \cos \omega t \, a_3 \cos \omega t \ldots], \tag{11}$$

writing the transpose of $\boldsymbol{q}$ for convenience. The corresponding added mass matrix may then be found, by expressing the coefficients $c_p$ in (6) in terms of the coefficients $a_p$.

The expression for $\phi$ in (5) is substituted into the boundary condition given by (4), by using the assumptions that $u = 0$ and $w$ is given by (9). This gives on $\nu = \nu_0$

$$\sum_{p=1}^{\infty} c_p T_p^1(\mu) \frac{\mathrm{d}U_p^1}{\mathrm{d}\nu} \frac{(\nu_0^2-1)^{\frac{1}{2}}}{\kappa(\nu_0^2-\mu^2)^{\frac{1}{2}}} \cos\theta \sin \omega t = \sum_{r=1}^{\infty} -\omega a_r T_r^1(\mu) \frac{a}{b} \frac{(\nu_0^2-1)^{\frac{1}{2}}}{(\nu_0^2-\mu^2)^{\frac{1}{2}}} \cos\theta \sin \omega t.$$

Next we multiply this equation by $T_s^1(\mu)$ and integrate over the range $-1 \leqslant \mu \leqslant 1$. Use of the orthogonality property of the functions $T_p^1(\mu)$, described in appendix A, leads to the result

$$c_p = -\omega a_p \frac{\kappa a}{b} \left(\frac{\mathrm{d}U_p^1}{\mathrm{d}\nu}\right)^{-1}_{\nu=\nu_0}. \tag{12}$$

The expression for kinetic energy in (6) therefore becomes, with $p$ replaced by $r$,

$$\begin{aligned} T_{\mathrm{f}} &= \tfrac{1}{2}\pi\rho_{\mathrm{f}} a b^2 \omega^2 \sum_{r=1}^{\infty} a_r^2 \left[\frac{-\nu_0 U_r^1(\nu_0)}{(\nu_0^2-1)\, U_r^{1\prime}(\nu_0)}\right] \frac{2r(r+1)}{2r+1} \sin^2 \omega t \\ &= \tfrac{1}{2}\dot{\boldsymbol{q}}' \overline{\boldsymbol{m}} \dot{\boldsymbol{q}}, \end{aligned} \tag{13}$$

where use has been made of the definition of $\boldsymbol{q}$ in (11). The corresponding added mass matrix, denoted $\overline{\boldsymbol{m}}$ in this case, is seen to be diagonal, with terms given by

$$\bar{m}_{rr} = \pi\rho_f ab^2 \frac{2r(r+1)}{2r+1}\left[\frac{-\nu_0 U_r^1(\nu_0)}{(\nu_0^2-1)\, U_r^{1\prime}(\nu_0)}\right], \quad r = 1, 2, \ldots. \tag{14}$$

We observe that this added mass matrix corresponds to generalized coordinates defined by (9) and (11). Only because the displacement $w$ has been expressed in terms of these particular 'modes' is this matrix diagonal. The modes are not strictly of physical significance, and it is fortuitous that they closely approximate the natural vibration modes of a solid spheroid of uniform density.

To obtain the three dimensional added mass correction factor $J_r$, corresponding to 'mode' $r$, we require the kinetic energy of the fluid in two dimensional motion. This may readily be shown to be

$$\begin{aligned}\bar{T}_f &= \tfrac{1}{2}\omega^2\pi\rho_f ab^2 \sum_{r=1}^{\infty}\sum_{s=1}^{\infty} a_r a_s \int_{-1}^{1} (1-\mu^2)\, w_r(\mu)\, w_s(\mu)\, \mathrm{d}\mu \sin^2\omega t \\ &= \tfrac{1}{2}\omega^2\pi\rho_f ab^2 \sum_{r=1}^{\infty} a_r^2 \frac{2r(r+1)}{2r+1}\sin^2\omega t. \end{aligned} \tag{15}$$

Hence the Lewis reduction factor $J_r^{\mathrm{L}}$ is given by

$$J_r^{\mathrm{L}} = \frac{T_f^{(r)}}{\bar{T}_f^{(r)}} = \left[\frac{-\nu_0 U_r^1(\nu_0)}{(\nu_0^2-1)\, U_r^{1\prime}(\nu_0)}\right], \tag{16}$$

where the superscript $r$ indicates the kinetic energy associated with 'mode' $r$.

### 2.3. *The motions assumed by Lockwood Taylor* (1930)

Consider next how this simple case is modified when it is desired to represent flexure of the body rather than deformation in shear: the added mass matrix thereby obtained is related to the three dimensional added mass reduction factors derived by Lockwood Taylor (1930) and discussed by Kruppa (1962). It is assumed that cross-sections normal to the neutral axis remain plane but rotate through the angle $\mathrm{d}w/\mathrm{d}x$. Hence points at radius $y$ on the surface of the body translate axially through the distance $u$ given by

$$u = -y\cos\theta\, \mathrm{d}w/\mathrm{d}x, \tag{17}$$

in addition to their lateral translation $w$. As before we take

$$w(\mu) = \sum_{r=1}^{\infty} a_r w_r(\mu)\cos\omega t.$$

We also now have

$$u(\mu,\theta) = \frac{-b}{a}\cos\theta \sum_{r=1}^{\infty} a_r (1-\mu^2)^{\frac{1}{2}} \frac{\mathrm{d}w_r(\mu)}{\mathrm{d}\mu}\cos\omega t. \tag{18}$$

If we substitute the expression for $\phi$ in (5) into (4), using (18), we obtain the result on $\nu = \nu_0$

$$\begin{aligned}&\sum_{p=1}^{\infty} c_p\, T_p^1(\mu) \frac{\mathrm{d}U_p^1}{\mathrm{d}\nu} \frac{(\nu_0^2-1)^{\frac{1}{2}}}{\kappa(\nu_0^2-\mu^2)^{\frac{1}{2}}}\cos\theta\sin\omega t \\ &\quad = \sum_{r=1}^{\infty} -\omega a_r \left[-\frac{b}{a}\mu\frac{\mathrm{d}w_r(\mu)}{\mathrm{d}\mu} + \frac{a}{b}w_r(\mu)\right](1-\mu^2)^{\frac{1}{2}} \frac{(\nu_0^2-1)^{\frac{1}{2}}}{(\nu_0^2-\mu^2)^{\frac{1}{2}}}\cos\theta\sin\omega t. \end{aligned}$$

This equation is simplified by multiplying throughout by $T_s^1(\mu)$ and integrating over the range $-1 \leqslant \mu \leqslant 1$. Using again the orthogonality property of the functions $T_p^1(\mu)$ given in appendix A, we find

$$c_p = -\omega \frac{\kappa a}{b} \left( \frac{\mathrm{d}U_p^1}{\mathrm{d}\nu} \right)^{-1}_{\nu=\nu_0} \sum_{r=1}^{\infty} D_{pr} a_r, \tag{19}$$

where

$$D_{pr} = \int_{-1}^{1} \left[ w_r(\mu) - \frac{b^2}{a^2} \mu \frac{\mathrm{d}w_r(\mu)}{\mathrm{d}\mu} \right] (1-\mu^2)^{\frac{1}{2}} T_p^1(\mu)\, \mathrm{d}\mu. \tag{20}$$

A new set of generalized coordinates may now be defined, so that analogous to (11) we have

$$\boldsymbol{q}^{*\prime} = [a_1^* \cos \omega t\, a_2^* \cos \omega t\, a_3^* \cos \omega t \ldots], \tag{21}$$

where the coefficients $a_p^*$ are defined by

$$a_p^* = \sum_{r=1}^{\infty} D_{pr} a_r, \quad p = 1, 2, \ldots. \tag{22}$$

Insertion of (19) into the expression for the fluid kinetic energy, in (6), leads to

$$T_{\mathrm{f}} = \tfrac{1}{2} \dot{\boldsymbol{q}}^{*\prime} \bar{\boldsymbol{m}} \dot{\boldsymbol{q}}^*, \tag{23}$$

where the added mass matrix is again given by (14). Note, however, that in this case $\bar{\boldsymbol{m}}$ corresponds to a different set of generalized coordinates $\boldsymbol{q}^*$. In terms of the original set, $\boldsymbol{q}$, the kinetic energy is

$$T_{\mathrm{f}} = \tfrac{1}{2} \dot{\boldsymbol{q}}' \boldsymbol{D}' \bar{\boldsymbol{m}} \boldsymbol{D} \dot{\boldsymbol{q}},$$

since the generalized coordinates are related by

$$\boldsymbol{q}^* = \boldsymbol{D}\boldsymbol{q},$$

where $\boldsymbol{D}$ is the matrix whose elements are $D_{pr}$. The added mass matrix $\boldsymbol{m}$ corresponding to the coordinates $\boldsymbol{q}$ is not now a diagonal matrix, when flexure of the body is represented. In fact

$$\boldsymbol{m} = \boldsymbol{D}' \bar{\boldsymbol{m}} \boldsymbol{D}. \tag{24}$$

To obtain the correction factors $J_r^{\mathrm{T}}$ corresponding to the Lockwood Taylor assumptions, we use the definition of $w_r(\mu)$ implied by (9). Distinguishing this case with a bar, we have

$$\bar{D}_{pr} = \int_{-1}^{1} \left[ T_r^1(\mu) - \frac{b^2}{a^2} \mu (1-\mu^2)^{\frac{1}{2}} \frac{\mathrm{d}}{\mathrm{d}\mu} \left( \frac{T_r^1(\mu)}{(1-\mu^2)^{\frac{1}{2}}} \right) \right] T_p^1(\mu)\, \mathrm{d}\mu.$$

The relations given in appendix A may be employed to provide the results

$$\bar{D}_{pr} = \begin{cases} 0, & p > r, \\ \left[ 1 - (r-1) \dfrac{b^2}{a^2} \right], & p = r, \\ -\tfrac{1}{2}(2p+1) \left[ 1 - (-1)^{p+r-1} \right] \dfrac{b^2}{a^2}, & p < r. \end{cases} \tag{25}$$

The kinetic energy of the fluid in two dimensional motion ($\bar{T}_{\mathrm{f}}$) must then be written in terms of the coordinates $\boldsymbol{q}^*$. This is because each factor $J_r^{\mathrm{T}}$ is associated by Lockwood Taylor with one

term of the series expansion for $\phi$ in (5). One term $c_p$ is therefore required, and this is associated with $q_p^*$ and not $q_p$, as seen from (19). By use of (15) $\overline{T}_f$ may therefore be expressed

$$\overline{T}_f = \tfrac{1}{2}\dot{\boldsymbol{q}}^{*\prime}\bar{\boldsymbol{E}}'\boldsymbol{R}\bar{\boldsymbol{E}}\dot{\boldsymbol{q}}^*, \tag{26}$$

where $\boldsymbol{R}$ is the diagonal matrix whose terms are

$$\boldsymbol{R}_{rr} = \frac{2r(r+1)}{2r+1}\pi\rho_f ab^2 \tag{27}$$

and the matrix $\bar{\boldsymbol{E}}$ is the inverse of $\bar{\boldsymbol{D}}$. Since $\bar{\boldsymbol{D}}$ is an upper triangular matrix, so also is $\bar{\boldsymbol{E}}$, and its terms are given by

$$\bar{E}_{pr} = \begin{cases} -\dfrac{1}{\bar{D}_{pp}} \displaystyle\sum_{q=p+2,\,p+4,\,\ldots}^{r} \bar{D}_{pq}\bar{E}_{qr}, & r-p = \text{any positive even integer}, \\ 0, & r-p = \text{any positive odd integer}, \\ \dfrac{1}{\bar{D}_{pp}}, & r = p, \\ 0, & r < p. \end{cases} \tag{28}$$

Using (8), (23) and (26), we obtain the Lockwood Taylor reduction factor $J_r^T$ given by

$$\left.\begin{aligned} J_r^T &= J_r^L \frac{R_{rr}}{\displaystyle\sum_{p=1}^{\infty} \bar{E}_{pr}^2 R_{pp}}, \\ &= J_r^L \frac{r(r+1)}{2r+1}\left[\sum_{p=1}^{r} \frac{p(p+1)}{2p+1}\bar{E}_{pr}^2\right]^{-1}, \end{aligned}\right\} \tag{29}$$

since the terms of the summation beyond $p = r$ are zero.

By use of these expressions it may be shown that the Lewis and Lockwood Taylor correction factors for the lowest few modes are related as follows

$$J_1^T = J_1^L,$$

$$J_2^T = J_2^L\left(1-\frac{b^2}{a^2}\right)^2,$$

$$J_3^T = J_3^L\left(1-2\frac{b^2}{a^2}\right)^2\left(1+\frac{7}{2}\frac{b^4}{a^4}\right)^{-1},$$

$$J_4^T = J_4^L\left(1-\frac{b^2}{a^2}\right)^2\left(1-3\frac{b^2}{a^2}\right)^2\left[\left(1-\frac{b^2}{a^2}\right)^2+\frac{27}{2}\frac{b^4}{a^4}\right]^{-1}.$$

Furthermore for very slender spheroids we may neglect the off-diagonal terms of matrix $\boldsymbol{D}$, and the Lockwood Taylor and Lewis factors may then be related by the simple expression

$$J_r^T = J_r^L\left[1-(r-1)\frac{b^2}{a^2}\right]^2. \tag{30}$$

We have thus found the relation between three dimensional correction factors for spheroids in motions characterized by flexure and shear. These two simple examples illustrate cases in which the added mass matrix for the spheroid may seemingly be found exactly. However the matrices so obtained are related to a set of generalized coordinates $q_r$ which are not of great use except for these particular cases. No physical meaning attaches to the coordinates, except for $a_1$ and $a_2$ which

correspond to amplitudes of heave and pitch respectively. Nor is this formulation readily applicable to the more general problem of a body whose surface is that of a spheroid, but whose density or elastic properties are non-uniform. Thus it is not clear how the Lewis and Lockwood Taylor approaches can be of direct help, if information is required about any modification to the three dimensional reduction factor for vibrations in the two node mode, resulting from significant asymmetry in the mode due to asymmetry in the inertia or stiffness of a ship hull. By generalizing the formulation, we may use a numerical method of finding characteristic modes and frequencies of a body, coupled with solution of the hydrodynamic problem and development of a 'physical' added mass matrix.

## 3. Finite element mass and stiffness matrices for a spheroid

### 3.1. *Structural mass and stiffness matrices*

The flexural modes and frequencies of a submerged spheroid, of variable density and elasticity, may be obtained within any reasonable degree of accuracy by the finite element method. The procedure is described in this and the following section of this paper. It is of value as an illustration of the manner in which the added mass matrix is derived and used for a more practical system of generalized coordinates than considered above. Furthermore it is felt that results obtained by this development may have wider application than to the very special case for which they are derived, which is the non uniform beam whose interface with the surrounding fluid is a spheroid.

The finite element method itself has been placed on a sound theoretical foundation which is well documented, for example by Zienkiewicz (1971). Results, however, for a spheroidal element have not apparently been published. This is due to the very specialized nature of such an element, its raison d'être being the spheroidal surface required for straightforward analysis of the fluid problem. We shall here first outline the development of consistent stiffness and mass matrices for non-uniform beam elements, and then give results for the special case when the element is a segment of a slender spheroid. The derivation follows that of Gallagher & Lee (1970) and is based on Euler–Bernoulli thin beam theory.

The beam is divided into $N$ elements by planes perpendicular to its axis. It is assumed that the vertical displacement $w$ within the $t$th beam element may be expressed in terms of the displacements and rotations at both ends (the finite element nodes for the beam element). Thus

$$\left.\begin{aligned} w(\xi) &= X_1(\xi)\, w_1^t + X_2(\xi)\, \theta_1^t + X_3(\xi)\, w_2^t + X_4(\xi)\, \theta_2^t \\ &= \boldsymbol{X}(\xi)\, \boldsymbol{q}_0^t, \end{aligned}\right\} \tag{31}$$

where $\xi$ is a non-dimensional coordinate along the neutral axis. The vector of nodal displacements is defined by

$$\boldsymbol{q}_0^t = \begin{bmatrix} w_1^t \\ \theta_1^t \\ w_2^t \\ \theta_2^t \end{bmatrix}.$$

The influence functions $X_i(\xi)$, $i = 1, \ldots, 4$ are those which render (31) the exact deflected shape for a uniform beam in static equilibrium under the action of end shears and moments. They are given in appendix B.

The kinetic energy $T$ of the element, of density $\rho_b$, area $A$, length $l$, is

$$T = \frac{1}{2}\int_0^1 A\rho_b \left(\frac{\partial w}{\partial t}\right)^2 l\,d\xi$$
$$= \tfrac{1}{2}\dot{\boldsymbol{q}}_0^{t\prime}\int_0^1 A\rho_b l\boldsymbol{X}'(\xi)\,\boldsymbol{X}(\xi)\,d\xi\,\dot{\boldsymbol{q}}_0^t.$$

Hence the mass matrix for the element is

$$\boldsymbol{M}^t = \int_0^1 A\rho_b l\boldsymbol{X}'(\xi)\boldsymbol{X}(\xi)\,d\xi. \tag{32}$$

The elastic strain energy $V$ of the element is

$$V = \frac{1}{2}\int_0^1 \frac{EI}{l^4}\left(\frac{\partial^2 w}{\partial \xi^2}\right)^2 l\,d\xi$$
$$= \tfrac{1}{2}\boldsymbol{q}_0^{t\prime}\int_0^1 \frac{EI}{l^3}\frac{d^2\boldsymbol{X}'}{d\xi^2}\frac{d^2\boldsymbol{X}}{d\xi^2}d\xi\,\boldsymbol{q}_0^t.$$

Hence the stiffness matrix for the element is

$$\boldsymbol{K}^t = \int_0^1 \frac{EI}{l^3}\frac{d^2\boldsymbol{X}'}{d\xi^2}\frac{d^2\boldsymbol{X}}{d\xi^2}d\xi. \tag{33}$$

These matrices have been evaluated by Gallagher & Lee for non-uniform beams whose sections vary according to

$$A = A_0(1+\sigma\xi^\alpha), \tag{34}$$

and

$$I = I_0(1+\tau\xi^\beta), \tag{35}$$

where $A_0$, $I_0$ are the cross-section area and moment of inertia at the element's left hand end. The geometry and sign convection is shown in figure 1*a*.

We require the appropriate matrices for the spheroidal element defined in figure 1*b*. Points in the element are defined by a dimensionless coordinate $\mu$ measured from the centre of the spheroid

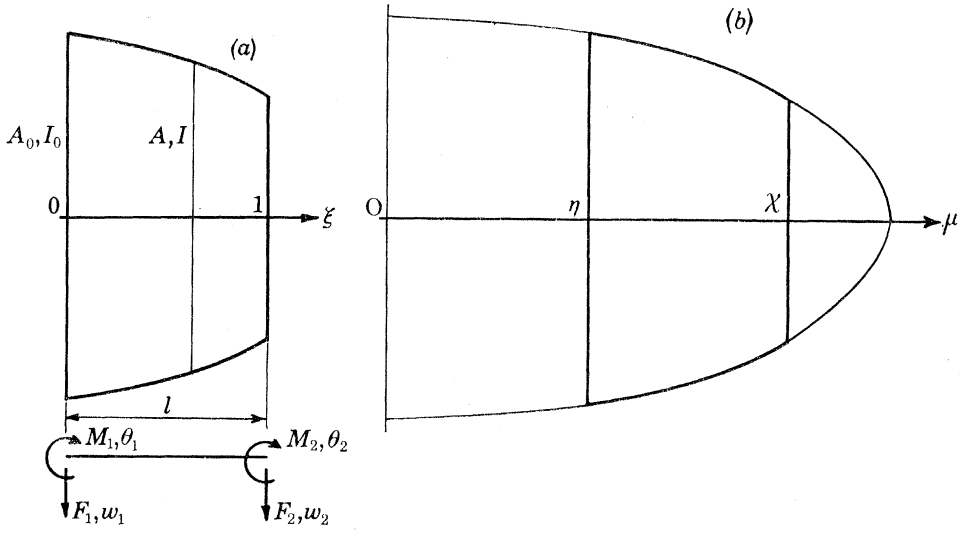


FIGURE 1. (*a*) Geometry and sign convention for non-uniform beam finite element. (*b*) Geometry of spheroidal element.

from which the segment is taken. The dimensionless coordinates of left and right hand ends are respectively $\eta$ and $\chi$. The major and minor semi-axes of the spheroid are $a$ and $b$, as before. Thus

$$A_0 = \pi b^2(1-\eta^2), \quad A = \pi b^2(1-\mu^2).$$

Therefore
$$A = A_0 \frac{1-\mu^2}{1-\eta^2}.$$

Similarly
$$I = I_0 \frac{(1-\mu^2)^2}{(1-\eta^2)^2}.$$

However
$$\xi = \frac{\mu-\eta}{\chi-\eta},$$

so that
$$\mu = \eta + (\chi-\eta)\,\xi. \tag{36}$$

This leads to
$$A = A_0\left[1 - \frac{2\eta(\chi-\eta)}{1-\eta^2}\xi - \frac{(\chi-\eta)^2}{1-\eta^2}\xi^2\right],$$

and
$$I = I_0\left[1 - \frac{2\eta(\chi-\eta)}{1-\eta^2}\xi - \frac{(\chi-\eta)^2}{1-\eta^2}\xi^2\right]^2.$$

Rather than (34) and (35) we need

$$A = A_0\Big(1 + \sum_{i=1,2} \sigma_i \xi^i\Big),$$

and
$$I = I_0\left(1 + \sum_{i=1}^{4} \tau_i \xi^i\right),$$

where
$$\sigma_1 = -\frac{2\eta(\chi-\eta)}{1-\eta^2}, \quad \text{etc.},$$

the other terms being given in appendix B. By using the results of Gallagher and Lee for $\alpha = 1, 2$ and $\beta = 1, 2, 3, 4$ it is a simple matter to obtain the appropriate matrices for the spheroidal element. These also are written out in appendix B.

These mass and stiffness matrices are element matrices corresponding to the two generalized coordinates at either end of the $t$th element, $w_1^t$, $\theta_1^t$, and $w_2^t$, $\theta_2^t$. The $(2N+2)$ generalized coordinates for the complete spheroid of $N$ elements are contained in the vector

$$\boldsymbol{q}_0' = (w_1^1\,\theta_1^1\,w_1^2\,\theta_1^2\,w_1^3\,\theta_1^3 \ldots w_1^{N+1}\theta_1^{N+1}).$$

The body mass matrix $\boldsymbol{M}$ and stiffness matrix $\boldsymbol{K}$ for the complete free–free spheroid are therefore square matrices of order $(2N+2)$; they are formed by assembling the element matrices along the principal diagonal, such that the first two rows and columns of the $t$th element matrix enter the same locations in the body matrix as the last two rows and columns of the $(t-1)$th matrix. This is a particularly straightforward example of the usual finite element procedure of forming overall mass and stiffness matrices from element matrices (Zienkiewicz 1971); in this case it is simplified by the fact that only two elements meet at a node, and by the free–free boundary condition.

### 3.2. *Hydrodynamic added mass and stiffness matrices*

The next step in this matrix formulation is to obtain hydrodynamic matrices corresponding to the finite element generalized coordinates $\boldsymbol{q}_0$. In this section we derive the added mass matrix $\boldsymbol{m}$ and added stiffness matrix $\boldsymbol{k}$ for a spheroid in fluid of density $\rho_f$.




PHILOSOPHICAL TRANSACTIONS OF THE ROYAL SOCIETY A MATHEMATICAL, PHYSICAL & ENGINEERING SCIENCES

We have shown that an added mass matrix for flexure of a spheroid may be obtained from

$$\boldsymbol{m} = \boldsymbol{D}'\bar{\boldsymbol{m}}\boldsymbol{D}, \qquad \text{((24) repeated)}$$

where the terms of matrix $\boldsymbol{D}$ are given by

$$D_{pr} = \int_{-1}^{1} \left[ w_r(\mu) - \frac{b^2}{a^2}\mu \frac{\mathrm{d}w_r(\mu)}{\mathrm{d}\mu} \right] (1-\mu^2)^{\frac{1}{2}}\, T_p^1(\mu)\, \mathrm{d}\mu \qquad \text{((20) repeated)}$$

and $\bar{\boldsymbol{m}}$ is obtained from (14). The terms of $\boldsymbol{m}$ correspond to as yet unspecified generalized coordinates implied by the displacements $w_r$. By relating the $w_r$ to the finite element coordinates $\boldsymbol{q}_0$, we may find the corresponding finite element matrix $\boldsymbol{m}$.

Within the $t$th element it is again assumed that a displacement $w$ may be written

$$w(\mu) = \boldsymbol{X}(\mu)\, \boldsymbol{q}_0^t.$$

This is (31) expressed in terms of the variable $\mu$, through the transformation of (36). We define $w_r(\mu)$ as the deflection function for the complete spheroid corresponding to a translation $w_1^t$ at node $t$, when all the other generalized coordinates in $\boldsymbol{q}_0$ are set to zero. Similarly we define $w_{r+1}(\mu)$ as the deflexion function corresponding to a rotation $\theta_1^t$. It is assumed that $r = 2t-1$. Then both $w_r(\mu)$ and $w_{r+1}(\mu)$ are zero everywhere except within the elements $t-1$ and $t$ on either side of node $t$ (at which point $\mu = \chi_{t-1} = \eta_t$). Thus

$$\left.\begin{aligned} w_r(\mu) &= X_3(\mu) \\ w_{r+1}(\mu) &= X_4(\mu) \end{aligned}\right\} \eta_{t-1} \leqslant \mu \leqslant \chi_{t-1}, \quad t = 2, \ldots, N+1,$$

$$\left.\begin{aligned} w_r(\mu) &= X_1(\mu) \\ w_{r+1}(\mu) &= X_2(\mu) \end{aligned}\right\} \eta_t \leqslant \mu \leqslant \chi_t, \quad t = 1, \ldots, N.$$

From these expressions the terms $D_{pr}$ of (20) may be evaluated.

With the exception of those terms corresponding to generalized displacements $w_1^1$, $\theta_1^1$, $w_1^{N+1}$, $\theta_1^{N+1}$, the terms in $\boldsymbol{D}$ involve contributions from two adjacent elements. The arrangement of the individual contributions in the complete matrix may be organized as follows. We assume that the infinite series hydrodynamic solution may be truncated at the term $p = P$, without significant loss of accuracy in determining the lowest modes. This assumption may be checked by convergence studies based on computed results. We may therefore construct a $P \times 4$ matrix $\boldsymbol{d}^t$ whose terms are given by

$$\mathrm{d}_{ps}^t = \pi ab \int_{\eta}^{\chi} \left[ X_s(\mu) - \frac{b^2}{a^2}\mu \frac{\mathrm{d}X_s(\mu)}{\mathrm{d}\mu} \right] (1-\mu^2)^{\frac{1}{2}}\, T_p^1(\mu)\, \mathrm{d}\mu. \qquad (37)$$

There will be one such $P \times 4$ matrix for each of the $N$ elements. For a particular displacement vector $\boldsymbol{q}_0$ there is a corresponding $4 \times 1$ element vector $\boldsymbol{q}_0^t$. The column of the matrix $\boldsymbol{D}$ which is associated with this $\boldsymbol{q}_0$ therefore corresponds to the equivalent column of the $P \times (2N+2)$ matrix $\boldsymbol{D}_0$ in

$$\boldsymbol{D}_0\boldsymbol{q}_0 = \sum_{t=1}^{N} \boldsymbol{d}^t \boldsymbol{q}_0^t. \qquad (38)$$

The $p$th row of $\boldsymbol{D}_0$ is formed by inserting the first two rows of $\boldsymbol{d}^t$ into the same locations as the second two rows of $\boldsymbol{d}^{t-1}$.

Finally the added mass matrix $\boldsymbol{m}$ associated with the finite element generalized coordinates $\boldsymbol{q}_0$ is given by

$$\boldsymbol{m} = \boldsymbol{D}_0'\bar{\boldsymbol{m}}\boldsymbol{D}_0. \qquad (39)$$



PHILOSOPHICAL TRANSACTIONS OF THE ROYAL SOCIETY A MATHEMATICAL, PHYSICAL & ENGINEERING SCIENCES

Evaluation of the terms of $\boldsymbol{m}$ is most simply achieved through use of certain recurrence relations for the generalized Legendre functions $T_p^1$ and $U_p^1$, described in appendix A. Each term involves the integral of a polynomial, which may in theory be obtained in closed form. However, because of the large number of terms in each polynomial when $P$ is large, the added mass matrices have here been computed by sixteen point Gaussian quadrature. The resulting integrations are 'exact' for polynomials up to degree 31, hence up to the terms given by $P = 29$. The matrix we obtain is consistent with the finite element mass matrix derived previously, and the two matrices $\boldsymbol{M}$ and $\boldsymbol{m}$ may be added to give a 'virtual mass' matrix for the submerged spheroid. For the floating spheroid, an approximation to the added mass matrix is $\frac{1}{2}\boldsymbol{m}$, and this must be added to $\boldsymbol{M}$ for the virtual mass matrix.†

Next let us consider the added stiffness matrix. The matrix we shall derive corresponds to the simple hydrostatic restoring forces associated with displacement of the spheroid from a position of equilibrium with its axis lying in the free surface. Such an approximation is consistent with that described above for the added mass matrix of a floating spheroid.

At a section of a body where the waterline beam is $2y$, the restoring force is $2\rho_f gy$ per unit displacement. The work done in a displacement $w$ of the section is $\frac{1}{2}(w^2)\,(2\rho_f gy)$. For the $t$th element the work done is

$$\int_0^1 w(\xi)^2 \rho_f gyl\,\mathrm{d}\xi = \tfrac{1}{2}\boldsymbol{q}_0^t\,\boldsymbol{k}^t\boldsymbol{q}_0^t,$$

where $\boldsymbol{k}^t$ is the added stiffness matrix given by

$$\boldsymbol{k}^t = \int_0^1 2\rho_f gyl\boldsymbol{X}'(\xi)\,\boldsymbol{X}(\xi)\,\mathrm{d}\xi. \tag{40}$$

This should be compared with (32) and (33) for the mass and stiffness matrices. For a spheroid in the coordinate system of figure 1*b*, this reduces to

$$\boldsymbol{k}^t = 2\rho_f gab\int_\eta^\chi (1-\mu^2)^{\frac{1}{2}}\,\boldsymbol{X}'(\mu)\,\boldsymbol{X}(\mu)\,\mathrm{d}\mu.$$

The terms of $\boldsymbol{k}^t$ may not be evaluated in closed form, because of the radical in the integrand. As for the terms of $\boldsymbol{d}^t$, they are here evaluated by sixteen point Gaussian quadrature. The total $(2N+2)\times(2N+2)$ added stiffness matrix $\boldsymbol{k}$ is then assembled in the same way as the stiffness matrix $\boldsymbol{K}$. The two may be added to obtain a 'virtual stiffness' matrix for the spheroid.

## 4. Characteristic modes and frequencies for variable density spheroids

Free flexural vibrations of the spheroid in an ideal fluid are governed by the equations

$$(\boldsymbol{K}+\boldsymbol{k})\,\boldsymbol{q}_0 - \omega^2(\boldsymbol{M}+\boldsymbol{m})\,\boldsymbol{q}_0 = 0. \tag{41}$$

We now proceed to evaluation of the eigenvalues and eigenvectors of this system of equations, for several examples. Thereby we illustrate the characteristics of the mode shapes and frequencies of submerged and floating bodies, the significance of distortions in the lowest two modes, and values of three dimensional added mass correction factors.

† Such an approximation is valid for the frequency range in which wave generation by the vibrating spheroid at the free surface may be neglected. The results of Kim (1965) suggest that for a rigid spheroid this corresponds to $\omega > 1.5\sqrt{(g/b)}$. In this range the free surface is approximately a surface of constant potential, and the flow approximates that around a spheroid in an infinite fluid. The added mass matrix however is obtained by integrating pressures only over the lower half of the spheroidal surface.

The accuracy of the results depends on the accumulation of round-off error in the numerical computations, and on the accuracy of the discrete idealization of the continuum problem. There was no evidence of numerical instability in any of the computations of results presented here, all of which were obtained by using double precision words on an I.B.M. 360/65 computer. It is thought that there is no significant error in any of these results due to round-off. The accuracy of the finite element idealization, and the significance of truncating the infinite series solution of the hydrodynamic problem, were investigated by convergence studies.

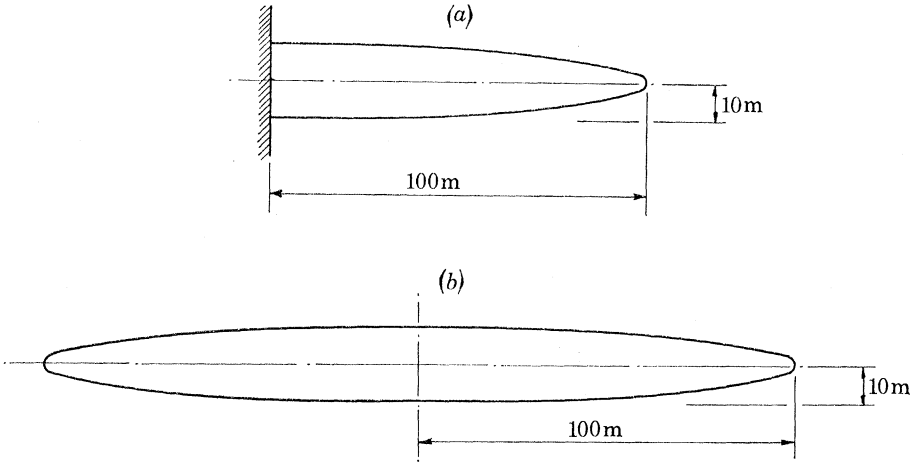


FIGURE 2. (*a*) $10 \times 1$ encastré half spheroid. (*b*) $10 \times 1$ free–free spheroid.

TABLE 1. CONVERGENCE STUDY OF A $10 \times 1$ ENCASTRÉ HALF SPHEROID *IN VACUO*

| number of elements, $N$ | $\omega_1$/min | $\omega_2$/min |
|---|---|---|
| 1 | 27.6576 | 127.034 |
| 2 | 27.6497 | 121.523 |
| 4 | 27.6462 | 121.180 |
| 'converged' frequencies, $\omega^c$ | 27.6449 | 121.158 |

It would be desirable to know whether the results obtained by means of the spheroidal finite element in fact converge to the 'correct' values. This should be tested by computing results for cases whose solutions may be found by other methods. It was hoped that it might be possible to check the formulation by calculating results for a spheroidal cantilever *in vacuo*. However, although closed form solutions for natural frequencies of several types of non-uniform cantilever may be found in the literature, this author has not yet been able to discover the case of the spheroid. Nevertheless, for possible future reference, natural frequencies were computed by this finite element formulation for a $10 \times 1$ half spheroid† encastré at the section of maximum area, as shown in figure 2*a*.

The eigenvalue analysis in this and subsequent computations was performed by using an I.B.M. subroutine based on the Jacobi method. The results are given in table 1, which refers to a spheroid of uniform density $\rho_b = 1000\,\mathrm{kg/m^3}$ and elastic modulus $E = 1000\,\mathrm{MPa}$, with half minor axis $b = 10.0\,\mathrm{m}$. All frequencies are in cycles per minute (c.p.m.). Results are given for 1, 2 and 4

† An $r \times 1$ spheroid is defined by $a/b = r$.

element idealizations, the elements in each case being of equal length, respectively 100, 50 and 25 m. The lowest frequencies $\omega_1$ and $\omega_2$ of this non-uniform cantilever are seen to converge very rapidly. We may obtain approximations to the 'converged' values using one of Richardson's extrapolation formulae (Salvadori & Baron 1961). To find the converged frequency $\omega^c$, using three results $\omega^{(1)}$, $\omega^{(2)}$ and $\omega^{(3)}$ from idealizations with $N_1$, $N_2$ and $N_3$ elements respectively, the appropriate formula is

$$\omega^c = \frac{N_1^4\omega^{(1)}}{(N_2^2-N_1^2)(N_3^2-N_1^2)} - \frac{N_2^4\omega^{(2)}}{(N_2^2-N_1^2)(N_3^2-N_2^2)} + \frac{N_3^4\omega^{(3)}}{(N_3^2-N_1^2)(N_3^2-N_2^2)}.$$

Applying this to the results of table 1 we obtain the 'converged' frequencies tabulated in the last row.

TABLE 2. CONVERGENCE STUDY OF $10 \times 1$ FREE-FREE SPHEROID DEEPLY SUBMERGED

| number of elements, $N$ | number of terms, $P$ | $\omega_1$/min | $\omega_2$/min | $J_1^*$ | $J_2^*$ |
|---|---|---|---|---|---|
| 2 | 8 | 29.0225 | 68.5939 | 0.82852 | 0.76516 |
| 4 | 5 | 28.9813 | 66.6810 | 0.82882 | 0.76382 |
| 4 | 8 | 28.9813 | 66.5307 | 0.82882 | 0.77183 |
| 4 | 12 | 28.9813 | 66.5304 | 0.82882 | 0.77185 |
| 8 | 5 | 28.9753 | 66.5446 | 0.82886 | 0.76372 |
| 8 | 8 | 28.9753 | 66.3833 | 0.82886 | 0.77227 |
| 'converged' frequencies, $\omega^c$ | | 28.9737 | 66.3669 | | |

If $EI_0$ and $m_0$ are the flexural rigidity and mass per unit length at the encastré end of a cantilever of length $l$, the natural frequencies may be expressed by

$$\omega_r^2 = k_r^2(EI_0/m_0 l^4)^{\frac{1}{2}}.$$

For the spheroid the converged frequencies lead to $k_1 = 2.406$, $k_2 = 5.037$. By comparison, the known solutions for a uniform cantilever are $k_1 = 1.875$, $k_2 = 4.694$.

Next a deeply submerged $10 \times 1$ free–free spheroid was examined. The geometry is indicated in figure 2*b*. The fluid density $\rho_f = 1000\,\mathrm{kg/m^3}$ and again $\rho_b = 1000\,\mathrm{kg/m^3}$, $E = 1000\,\mathrm{MPa}$. The results for several idealizations are given in table 2. Consider first the solutions which use 8 terms in the series of associated Legendre frunctions for the hydrodynamic analysis ($P = 8$). Results are given for cases with 2, 4 and 8 equal length elements. The frequencies $\omega_1$ and $\omega_2$, corresponding to two and three node modes of flexural vibration of the free–free spheroid, also converge rapidly.† Using the extrapolation formula again, we obtain the converged frequencies given in the last row of table 2. These figures suggest that the 4 element idealization gives results that are within 0.03 % and 0.3 % of the 'correct' values for $\omega_1$ and $\omega_2$ respectively. Subsequent results are therefore all based on representation by four finite elements, since we are at this stage interested only in the lowest modes ($r = -1, 0, 1, 2$).

Consider next the values in table 2 computed from the 4 element idealization of the $10 \times 1$ spheroid, using 5, 8 and 12 terms in the series of associated Legendre functions. Within six figure accuracy $\omega_1$ is unchanged by using more terms than 5; $\omega_2$ is decreased by 3 in the sixth significant digit if 12 instead of 8 terms are included. These findings suggest that 8 terms are sufficient, and this was assumed in obtaining subsequent results reported herein.

Among these results are values computed for a three dimensional reduction factor $J_r^*$ for the

† Note that for a free–free beam it is convenient to associate the lowest two modes with $r = -1, 0$. For a beam *in vacuo* these are rigid modes.

$r$th characteristic mode. This is defined as the ratio of (kinetic energy of fluid in three dimensional (3D) motion for a mode shape calculated assuming 3D motion) to (kinetic energy of fluid in two dimensional (2D) motion for the same mode shape). An alternative definition would have as the quotient (kinetic energy of fluid in 2D motion for a mode shape calculated assuming 2D motion). For a uniform spheroid the resulting values of $J_r^*$ would be almost identical, since the mode shapes are virtually the same. For a non-uniform spheroid, it is arguable that neither definition is more logical than the other, since a third definition of the quotient might be (kinetic energy of fluid in 2D motion for a mode shape calculated assuming 2D motion and the correct $J_r^*$ value). The difficulty arises because the distribution of 2D added mass will generally differ from the non-uniform spheroid mass distribution; hence different $J$ values will lead to different mode shapes, but the correct mode shape is not known before $J$ has been evaluated. These differences are small for a slender beam, but they underline the inconsistencies in use of a three dimensional correction factor applied to a two dimensional added mass distribution. A rational approach requires a full three dimensional analysis throughout. We have here used the first definition given above, since the three dimensionality of the flow is most clearly illustrated by comparing results for motions following the same modal pattern.

TABLE 3. THREE DIMENSIONAL REDUCTION FACTORS $J_r$ FOR DEEPLY SUBMERGED SPHEROIDS

| | | Lewis factor $J_r^L$ | | L. Taylor factor $J_r^T$ | | f.e.m. factor $J_r^*$ |
|---|---|---|---|---|---|---|
| spheroid | mode† | present values | values in Todd (1962) | present values | values in Todd (1962) | 4 elements 8 terms |
| $10 \times 1$ | $-1$ | 0.9602 | — | 0.9602 | — | 0.960 |
| | 0 | 0.9105 | — | 0.8924 | — | 0.892 |
| | 1 | 0.8586 | 0.858 | 0.8243 | 0.825 | 0.829 |
| | 2 | 0.8080 | 0.811 | 0.7592 | 0.760 | 0.772 |
| $8 \times 1$ | $-1$ | 0.9447 | — | 0.9447 | — | 0.945 |
| | 0 | 0.8798 | — | 0.8525 | — | 0.853 |
| | 1 | 0.8155 | 0.818 | 0.7647 | 0.764 | 0.772 |
| | 2 | 0.7557 | 0.758 | 0.6842 | 0.682 | 0.704 |
| $6 \times 1$ | $-1$ | 0.9171 | — | 0.9171 | — | 0.917 |
| | 0 | 0.8289 | — | 0.7835 | — | 0.783 |
| | 1 | 0.7483 | 0.752 | 0.6656 | 0.674 | 0.678 |
| | 2 | 0.6779 | 0.675 | 0.5634 | 0.564 | 0.599 |
| $4 \times 1$ | $-1$ | 0.8598 | — | 0.8598 | — | 0.860 |
| | 0 | 0.7349 | — | 0.6459 | — | 0.646 |
| | 1 | 0.6349 | — | 0.4795 | — | 0.508 |
| | 2 | 0.5558 | — | 0.3462 | — | 0.426 |

† Note that for the free–free spheroids the modes are numbered in an order corresponding to the notation of heave ($-1$), pitch (0), two node vertical (1) and three node vertical (2).

The values of $J_r^*$ for modes 1 and 2 of the $10 \times 1$ deeply submerged spheroid are indicated in table 2, calculated from the several idealizations. Results of the four element eight term idealization again appear to have converged, to the third significant digit.

A by-product of computation of the added mass matrix for the spheroid, through use of the recurrence relations in appendix A, is a set of values of Lewis and Lockwood Taylor factors $J_r^L$ and $J_r^T$. These are given by (16) and (29) respectively. The results for modes $-1$, 0, 1 and 2 of four uniform submerged spheroids are given in table 3. Tabulated alongside are some values

quoted by Todd (1961), and values of $J_r^*$ computed by the finite element method according to the first definition above. It is apparent that the figures given by Todd are not all identical to the corresponding values computed here, but this is probably due to small errors introduced into manual calculations of the earlier figures. More significant is the difference between the values of $J_r^{\mathrm{T}}$ and $J_r^*$, particularly for the spheroids of shorter length to breadth ratio. In both cases flexural rotation of cross-sections is assumed (in contrast to the calculation of $J_r^{\mathrm{L}}$), but $J_r^*$ is based on a reasonably precise evaluation of flexural mode shape. The derivation of $J_r^{\mathrm{T}}$, based on simple polynomial modes, in all cases overestimates the three dimensionality of the flow. It appears that this effect would be considerable in the higher modes; furthermore the discrepancy would presumably be greater still if the calculation allowed for significant shear deformation in the higher modes. In the $-1$ mode, however, in which there is no cross-section rotation during submerged motions, the values of $J_{-1}^{\mathrm{L}}$, $J_{-1}^{\mathrm{T}}$ and $J_{-1}^*$ should clearly be identical: the computed results in table 3 confirm this.

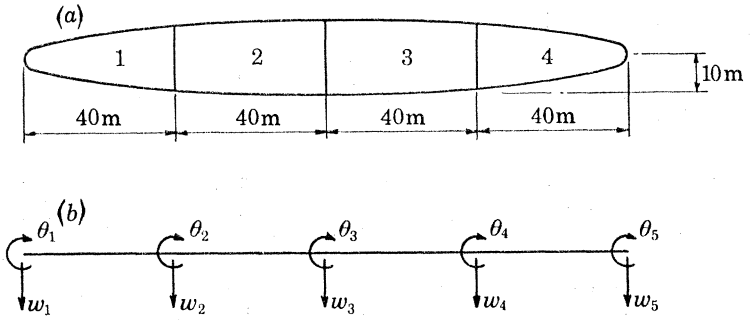


FIGURE 3. (*a*) Numbering scheme and geometry for $8 \times 1$ spheroid examples.
(*b*) Degrees of freedom for four-element idealization.

TABLE 4. PROPERTIES OF $8 \times 1$ SPHEROID EXAMPLES

| spheroid type | element density†/kg m$^{-3}$ | | | |
|---|---|---|---|---|
| | element 1 | element 2 | element 3 | element 4 |
| A | 1000 | 1000 | 1000 | 1000 |
| B | 2100 | 500 | 500 | 2100 |
| C | 500 | 500 | 500 | 3700 |

fluid density = 1000 kg/m$^3$.

† Element densities are halved for floating spheroids.

The influence of mode shapes on $J_r^*$ has been examined by performing calculations for three different $8 \times 1$ spheroids. The first, A, is of uniform density; B is symmetric about the mid point, but the element at either end is denser than the centre elements; C is unsymmetric, an element at one end being denser than the other three. All three spheroids have the same total mass. Their properties are described in figure 3*a* and table 4. Their dimensions were selected to provide frequencies of the same order as those of a very large tanker or Great Laker. Nine cases were analysed, as indicated in table 5, corresponding to vibrations *in vacuo*, deeply submerged, and floating. The elastic modulus of the spheroids was the same in all cases with the exception of case 4, in which $E$ was reduced by a factor of five to investigate the characteristics of the lowest modes of a more flexible body. The two values of modulus which were chosen lead to natural frequencies of the floating spheroid slightly higher and slightly lower than those of a typical 200 000 tonnes

PHILOSOPHICAL TRANSACTIONS OF THE ROYAL SOCIETY A MATHEMATICAL, PHYSICAL & ENGINEERING SCIENCES



TABLE 5. MODE SHAPES, FREQUENCIES AND THREE DIMENSIONAL REDUCTION FACTORS FOR $8 \times 1$ SPHEROIDS

| case no. | spheroid type | configuration | modulus, $E$ / MPa | mode no. | $\omega_r$ / min | $J^*$ | mode shape (all values of $\theta$ must be multiplied by $10^{-2}$) $w_1$ | $\theta_1$ | $w_2$ | $\theta_2$ | $w_3$ | $\theta_3$ | $w_4$ | $\theta_4$ | $w_5$ | $\theta_5$ |
|---|---|---|---|---|---|---|---|---|---|---|---|---|---|---|---|---|
| 1 | A | *in vacuo* | 1000 | −1 | 0 | — | 0.4472 | 0 | 0.4472 | 0 | 0.4472 | 0 | 0.4472 | 0 | 0.4472 | 0 |
| | | | | 0 | 0 | — | −0.6324 | 0.3953 | −0.3162 | 0.3953 | 0 | 0.3953 | 0.3162 | 0.3953 | 0.6324 | 0.3953 |
| | | | | 1 | 30.62 | — | 0.6904 | −0.8899 | 0.0580 | −0.6147 | −0.1996 | 0 | 0.0580 | 0.6147 | 0.6904 | 0.8899 |
| | | | | 2 | 69.19 | — | −0.6950 | 1.5089 | 0.1296 | 0.4001 | 0 | −0.4696 | −0.1296 | 0.4001 | 0.6950 | 1.5089 |
| 2 | A | submerged | 1000 | −1 | 0 | 0.9447 | 0.4472 | 0 | 0.4472 | 0 | 0.4472 | 0 | 0.4472 | 0 | 0.4472 | 0 |
| | | | | 0 | 0 | 0.8525 | −0.6324 | 0.3953 | −0.3162 | 0.3953 | 0 | 0.3953 | 0.3162 | 0.3953 | 0.6324 | 0.3953 |
| | | | | 1 | 23.00 | 0.7718 | 0.6904 | −0.8776 | 0.0613 | −0.6158 | −0.1973 | 0 | 0.0613 | 0.6158 | 0.6904 | 0.8776 |
| | | | | 2 | 53.00 | 0.7039 | −0.6958 | 1.4741 | 0.1250 | 0.4090 | 0 | −0.4667 | 0.1250 | 0.4090 | 0.6958 | 1.4741 |
| 3 | A | floating | 1000 | −1 | 5.87 | 0.9452 | 0.4385 | 0.0203 | 0.4514 | 0.0114 | 0.4560 | 0 | 0.4514 | −0.0114 | 0.4385 | −0.0203 |
| | | | | 0 | 6.72 | 0.8528 | −0.6314 | 0.3866 | −0.3183 | 0.3955 | 0 | 0.3992 | 0.3183 | 0.3955 | 0.6314 | 0.3866 |
| | | | | 1 | 33.32 | 0.7715 | 0.6904 | −0.8712 | 0.0631 | −0.6163 | −0.1960 | 0 | 0.0631 | 0.6163 | 0.6904 | 0.8712 |
| | | | | 2 | 75.33 | 0.7038 | −0.6959 | 1.4705 | 0.1246 | 0.4101 | 0 | −0.4666 | −0.1246 | 0.4101 | 0.6959 | 1.4705 |
| 4 | A | floating | 200 | −1 | 5.84 | 0.9466 | 0.4037 | 0.0977 | 0.4664 | 0.0555 | 0.4889 | 0 | 0.4664 | −0.0555 | 0.4037 | −0.0977 |
| | | | | 0 | 6.71 | 0.8538 | −0.6270 | 0.3516 | −0.3269 | 0.3963 | 0 | 0.4149 | 0.3269 | 0.3963 | 0.6270 | 0.3516 |
| | | | | 1 | 16.25 | 0.7709 | 0.6904 | −0.8461 | 0.0700 | −0.6187 | −0.1913 | 0 | 0.0700 | 0.6187 | 0.6904 | 0.8461 |
| | | | | 2 | 34.35 | 0.7033 | −0.6962 | 1.4559 | 0.1228 | 0.4144 | 0 | −0.4660 | −0.1228 | 0.4144 | 0.6962 | 1.4559 |
| 5 | B | *in vacuo* | 1000 | −1 | 0 | — | 0.4472 | 0 | 0.4472 | 0 | 0.4472 | 0 | 0.4472 | 0 | 0.4472 | 0 |
| | | | | 0 | 0 | — | −0.6324 | 0.3953 | −0.3162 | 0.3953 | 0 | 0.3953 | 0.3162 | 0.3953 | 0.6324 | 0.3953 |
| | | | | 1 | 28.15 | — | 0.6540 | −1.0899 | −0.0860 | −0.6751 | −0.3597 | 0 | −0.0860 | 0.6751 | 0.6540 | 1.0899 |
| | | | | 2 | 63.36 | — | 0.6796 | −1.8692 | −0.1943 | −0.2512 | 0 | 0.4863 | 0.1943 | −0.2512 | −0.6796 | −1.8692 |
| 6 | B | submerged | 1000 | −1 | 0 | 0.9447 | 0.4472 | 0 | 0.4472 | 0 | 0.4472 | 0 | 0.4472 | 0 | 0.4472 | 0 |
| | | | | 0 | 0 | 0.8525 | −0.6324 | 0.3953 | −0.3162 | 0.3953 | 0 | 0.3953 | 0.3162 | 0.3953 | 0.6324 | 0.3953 |
| | | | | 1 | 20.81 | 0.8020 | 0.6791 | −0.9824 | −0.0092 | −0.6527 | −0.2781 | 0.0 | −0.0092 | 0.6527 | 0.6791 | 0.9824 |
| | | | | 2 | 49.51 | 0.7244 | 0.6857 | −1.6992 | −0.1717 | −0.3223 | 0 | 0.4931 | 0.1717 | −0.3223 | −0.6857 | −1.6992 |
| 7 | B | floating | 1000 | −1 | 5.86 | 0.9446 | 0.4493 | −0.0006 | 0.4465 | −0.0047 | 0.4445 | 0 | 0.4465 | 0.0047 | 0.4493 | 0.0006 |
| | | | | 0 | 5.76 | 0.8526 | −0.6320 | 0.3898 | −0.3171 | 0.3962 | 0 | 0.3963 | 0.3171 | 0.3962 | 0.6320 | −0.3898 |
| | | | | 1 | 30.13 | 0.8025 | 0.6788 | −0.9802 | −0.0098 | −0.6542 | −0.2794 | 0 | −0.0098 | 0.6542 | 0.6788 | 0.9802 |
| | | | | 2 | 70.34 | 0.7243 | 0.6857 | −1.6977 | −0.1716 | −0.3225 | 0 | 0.4930 | 0.1716 | −0.3225 | −0.6857 | −1.6977 |
| 8 | C | *in vacuo* | 1000 | −1 | 0 | — | 0.4472 | 0 | 0.4472 | 0 | 0.4472 | 0 | 0.4472 | 0 | 0.4472 | 0 |
| | | | | 0 | 0 | — | 0.7634 | −0.3567 | 0.4780 | −0.3567 | 0.1926 | −0.3567 | −0.0927 | −0.3567 | −0.3781 | −0.3567 |
| | | | | 1 | 31.68 | — | −0.7890 | 0.8648 | −0.1462 | 0.6876 | 0.2320 | 0.2168 | 0.1437 | −0.4731 | −0.5304 | −1.1304 |
| | | | | 2 | 66.45 | — | −0.7724 | 1.2959 | 0.0594 | 0.6448 | 0.1673 | −0.3082 | −0.1381 | −0.1306 | 0.5934 | 2.0882 |
| 9 | C | submerged | 1000 | −1 | 0 | 0.9447 | 0.4472 | 0 | 0.4472 | 0 | 0.4472 | 0 | 0.4472 | 0 | 0.4472 | 0 |
| | | | | 0 | 0 | 0.8646 | −0.7208 | 0.3839 | −0.4137 | 0.3839 | −0.1066 | 0.3839 | 0.2005 | 0.3839 | 0.5076 | 0.3839 |
| | | | | 1 | 22.22 | 0.7951 | −0.7782 | 0.8916 | −0.1185 | 0.6898 | 0.2330 | 0.1479 | 0.0801 | −0.5360 | −0.5652 | −0.9870 |
| | | | | 2 | 50.51 | 0.7177 | 0.7207 | −1.3094 | −0.0866 | −0.5442 | −0.0868 | 0.4103 | 0.1749 | −0.0885 | −0.6590 | −1.9779 |

dead weight tanker. The results in table 5 give for the lowest modes ($r = -1, 0, 1, 2$) the natural frequencies $\omega_r$, values of the factor $J_r^*$, and mode shapes expressed in terms of the ten degrees of freedom of the four finite element idealization shown in figure 3*b*.

Some of the mode shapes have been plotted in figure 4 and figure 5. To achieve reasonable accuracy it was necessary to compute values of the deflexion curves at intermediate points between the finite element nodes. This however was a simple matter, since the deflexion at any point within an element may be expressed in terms of the nodal displacements $w$ and $\theta$ at either end, by using (31). Modes $-1$ and 0 of the symmetric spheroids *in vacuo* and deeply submerged

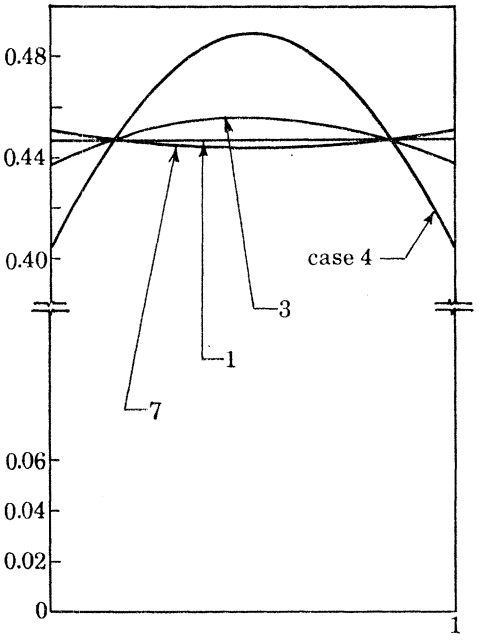


FIGURE 4. Shapes of $-1$ mode ('heave') for submerged and floating spheroids.

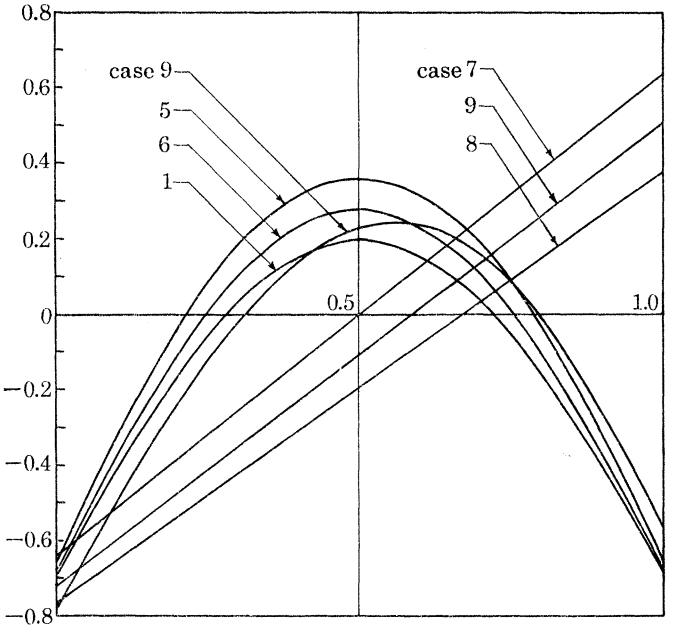


FIGURE 5. Shapes of modes 0 and 1 for spheroids *in vacuo*, submerged, and floating.

are true rigid body modes (see cases 1, 2, 5 and 6). The corresponding modes of the floating bodies show evidence of distortions (cases 3, 4 and 7), the relative magnitudes of which are compared in figure 4 for the 'heave' mode. Even if account is taken of the exaggeration introduced by the false origin in figure 4, the amount of distortion in this so-called 'rigid' mode is surprising. Assessing relative flexibilities by reference to 'two node' natural frequencies, we can postulate that the $-1$ mode of a 200 000 td.wt tanker having $\omega_1 = 27\ \mathrm{min}^{-1}$ may lie between the curves in figure 4 which represent cases 3 and 4 (corresponding to $\omega_1 = 32\ \mathrm{min}^{-1}$ and $\omega_1 = 22\ \mathrm{min}^{-1}$ respectively). The possibility of this amount of distortion in the 'rigid' mode of a real ship is a matter which should be investigated further: in the case of very large ships, this will probably be influenced by wave generation at the free surface, an effect which has of course been neglected here. Another important influence is illustrated in figure 4: comparing the mode shapes for cases 3 and 7 we see the very marked effect of varying the distribution of mass along a ship. This also influences the natural frequencies of the lowest two modes of the floating spheroids. Comparing cases 3 and 7 in table 5 we see that the order of modes is reversed: for the uniform spheroid the lowest frequency corresponds to heaving (with distortion), whereas for case 7 the pitching frequency is lowest.

One of the truly rigid modes of beams *in vacuo* or deeply submerged is also influenced by mass distribution. We are referring of course to the influence of asymmetry, which shifts the axis about which pitching occurs. This is illustrated in figure 5. Mode 0 is indicated for cases 1 (symmetric *in vacuo*), 8 (unsymmetric *in vacuo*) and 9 (unsymmetric submerged). The presence of a fluid decreases the asymmetry, shifting the axis of rotation back towards the mid point of the beam.

Also shown in figure 5 are the two node vibration modes for cases 1, 5, 6 and 9. We see from table 5 that of the nine cases these four represent the significantly different shapes of mode 1. Case 1 is very similar to cases 2, 3 and 4; case 6 is close to case 7; and case 8 does not differ greatly from case 9. But the various shapes clearly lead to different values of $J_1^*$, the three dimensional reduction factor for the $8 \times 1$ spheroid in mode 1. The maximum variation is 4 %, compared with 7 % between the corresponding Lockwood Taylor and Lewis $J$ values.

Some of the conclusions we may draw from these results are the following:

(1) Consistent mass and added mass matrices may effectively be combined to yield characteristic modes and frequencies of submerged bodies. With the inclusion of an approximate added stiffness matrix in the formulation, derived by a consistent approach to the buoyancy forces, floating bodies may also be analysed.

(2) Very accurate calculation of three dimensional reduction factors is not worthwhile, since these factors depend on characteristic mode shapes which vary with structural properties. It should however be noted that the values quoted in some of the literature appear to contain some slight numerical inaccuracies.

(3) The lowest mode of symmetric motion of a ship (namely in a vertical plane) may theoretically be pitch or heave, depending on waterline and mass distribution.

(4) The lowest two modes of relatively flexible ships, such as tankers and Great Lakers, may entail significant distortion of the neutral axis.

(5) The results obtained here may be used to assess the accuracy of approximate techniques for bodies of more complicated configuration. The next stage is to combine a three dimensional finite element representation of the structure with a numerical model of the three dimensional flow past more complex geometries than the spheroid. Methods under investigation involve fluid finite elements, and distributed singularities on or near the body surface.



PHILOSOPHICAL TRANSACTIONS OF THE ROYAL SOCIETY A MATHEMATICAL, PHYSICAL & ENGINEERING SCIENCES

## Appendix A. Properties of generalized Legendre functions

Our derivation of the added mass matrix for a spheroidal element makes use of certain properties of generalized Legendre functions, $T_p^m$ and $U_p^m$. These are described by the following relations, which are based on results in Erdélyi (1953).

The functions $w = T_p^m(z)$ and $w = U_p^m(z)$ are solutions of Legendre's differential equation

$$(1-z^2)\frac{\mathrm{d}^2 w}{\mathrm{d}z^2} - 2z\frac{\mathrm{d}w}{\mathrm{d}z} + \left[p(p+1) - \frac{m^2}{1-z^2}\right] w = 0.$$

They satisfy

$$T_p^m(z) = (1-z^2)^{\frac{1}{2}m}\frac{\mathrm{d}^m P_p(z)}{\mathrm{d}z}, \quad p \geqslant m,$$

and

$$U_p^m(z) = (z^2-1)^{\frac{1}{2}m}\frac{\mathrm{d}^m Q_p(z)}{\mathrm{d}z}, \quad p \geqslant m,$$

where $P_p$ and $Q_p$ are respectively Legendre polynomials of the first and second kind of degree $p$. The generalized functions $T_p^m$ and $U_p^m$ obey the recurrence relations

$$(p-m+1)\, T_{p+1}^m(z) = (2p+1)\, z T_p^m(z) - (p+m)\, T_{p-1}^m(z)$$

and

$$(p-m+1)\, U_{p+1}^m(z) = (2p+1)\, z U_p^m(z) - (p+m)\, U_{p-1}^m(z).$$

We require these functions for the case $m = 1$, and $p =$ any positive integer. They may be found by using the above recurrence relations and the expressions

$$T_1^1(z) = (1-z^2)^{\frac{1}{2}},$$

$$T_2^1(z) = 3z(1-z^2)^{\frac{1}{2}},$$

$$U_1^1(z) = \left[\tfrac{1}{2}\lg\frac{z+1}{z-1} - \frac{z}{z^2-1}\right](z^2-1)^{\frac{1}{2}},$$

$$U_2^1(z) = \left[\tfrac{3}{2}z\lg\frac{z+1}{z-1} - 3 - \frac{1}{z^2-1}\right](z^2-1)^{\frac{1}{2}}.$$

We also require the relation

$$(z^2-1)\frac{\mathrm{d}U_p^m(z)}{\mathrm{d}z} = pzU_p^m(z) - (p+m)\, U_{p-1}^m(z).$$

With $m = 1$, this leads to

$$\frac{-zU_p^1(z)}{(z^2-1)\, U_p^{1\prime}(z)} = \left[(p+1)\,\frac{U_{p-1}^1(z)}{zU_p^1(z)} - p\right]^{-1},$$

which is needed in evaluating the added mass matrix. The special case of $p = 1$ is given by

$$\frac{-U_1^1 z(z)}{(z^2-1)\, U_1^{1\prime}(z)} = 2\left[\tfrac{1}{2}z(z^2-1)\lg\frac{z+1}{z-1} - (z^2-2)\right]^{-1} - 1.$$

All these expressions may be calculated by simple subroutines, for appropriate values of $z$ and any positive integer $p$.

The generalized Legendre functions of the first kind also satisfy the orthogonality relations

$$\int_{-1}^{1} T_p^m(\mu)\, T_r^m(\mu)\, \mathrm{d}\mu = \begin{cases} \dfrac{(p+m)!}{(p-m)!}\dfrac{2}{2p+1}, & p = r \\ 0, & p \neq r \end{cases}$$

where $m = 1, 2, \ldots$ with $m \leqslant p$.

## Appendix B. Details of spheroid mass and stiffness matrices

This appendix lists the numerical expressions to which reference is made in § 3.1.

The influence functions $X_i(\xi)$ are given by

$$X_1(\xi) = (1+2\xi)(\xi-1)^2,$$

$$X_2(\xi) = \xi(\xi-1)^2,$$

$$X_3(\xi) = \xi^2(3-2\xi),$$

$$X_4(\xi) = \xi^2(\xi-1).$$

The area $A$ of the spheroidal element at section $\xi$ is expressed in terms of the area of the left hand end $A_0$ (see figure 1*b*) by

$$A = A_0\Big(1+\sum_{i=1,2}\sigma_i\xi^i\Big),$$

where

$$\sigma_1 = -\frac{2\eta(\chi-\eta)}{1-\eta^2},$$

and

$$\sigma_2 = -\frac{(\chi-\eta)^2}{1-\eta^2}.$$

The moment of inertia $I$ at section $\xi$ is expressed in terms of the inertia $I_0$ at the left hand end by

$$I = I_0\Big(1+\sum_{i=1}^{4}\tau_i\xi^i\Big),$$

where

$$\tau_1 = -\frac{4\eta(\chi-\eta)}{1-\eta^2},$$

$$\tau_2 = \frac{2(3\eta^2-1)(\chi-\eta)^2}{(1-\eta^2)^2},$$

$$\tau_3 = \frac{4\eta(\chi-\eta)^3}{(1-\eta^2)^2},$$

$$\tau_4 = \frac{(\chi-\eta)^4}{(1-\eta^2)^2}.$$

The mass and stiffness matrices of the spheroidal element, $\boldsymbol{M}^t$ and $\boldsymbol{K}^t$ respectively, are given by the definitions which follow.

PHILOSOPHICAL TRANSACTIONS OF THE ROYAL SOCIETY A MATHEMATICAL, PHYSICAL & ENGINEERING SCIENCES



$$M^t = \rho_b A_0 l \begin{bmatrix} (\frac{13}{35}+\frac{3}{35}\sigma_1+\frac{19}{630}\sigma_2) & (\frac{11}{210}+\frac{1}{60}\sigma_1+\frac{17}{2520}\sigma_2)\,l & (\frac{9}{70}+\frac{9}{140}\sigma_1+\frac{23}{630}\sigma_2) & -(\frac{13}{420}+\frac{1}{70}\sigma_1+\frac{19}{2520}\sigma_2)\,l \\ & (\frac{1}{105}+\frac{1}{280}\sigma_1+\frac{1}{630}\sigma_2)\,l^2 & (\frac{13}{420}+\frac{1}{60}\sigma_1+\frac{5}{504}\sigma_2)\,l & -(\frac{1}{140}+\frac{1}{280}\sigma_1+\frac{1}{504}\sigma_2)\,l^2 \\ & & (\frac{13}{35}+\frac{2}{7}\sigma_1+\frac{29}{126}\sigma_2) & -(\frac{11}{210}+\frac{1}{28}\sigma_1+\frac{13}{504}\sigma_2\,l \\ & \text{symmetric} & & (\frac{1}{105}+\frac{1}{168}\sigma_1+\frac{1}{252}\sigma_2)\,l^2 \end{bmatrix}$$

$$K^t = \frac{EI_0}{l^3} \begin{bmatrix} 12(1+\frac{1}{2}\tau_1+\frac{2}{5}\tau_2+\frac{7}{20}\tau_3+\frac{11}{35}\tau_4) & 6l(1+\frac{1}{3}\tau_1+\frac{7}{30}\tau_2+\frac{1}{5}\tau_3+\frac{19}{105}\tau_4) & -12(1+\frac{1}{2}\tau_1+\frac{2}{5}\tau_2+\frac{7}{20}\tau_3+\frac{11}{35}\tau_4) & 6l(1+\frac{2}{3}\tau_1+\frac{17}{30}\tau_2+\frac{1}{2}\tau_3+\frac{47}{105}\tau_4) \\ & 4l^2(1+\frac{1}{4}\tau_1+\frac{2}{15}\tau_2+\frac{1}{10}\tau_3+\frac{3}{35}\tau_4) & -6l(1+\frac{1}{3}\tau_1+\frac{7}{30}\tau_2+\frac{1}{5}\tau_3+\frac{19}{105}\tau_4) & 2l^2(1+\frac{1}{2}\tau_1+\frac{13}{30}\tau_2+\frac{2}{5}\tau_3+\frac{13}{35}\tau_4) \\ & & 12(1+\frac{1}{2}\tau_1+\frac{2}{5}\tau_2+\frac{7}{20}\tau_3+\frac{11}{35}\tau_4) & -6l(1+\frac{2}{3}\tau_1+\frac{17}{30}\tau_2+\frac{1}{2}\tau_3+\frac{47}{105}\tau_4) \\ & \text{symmetric} & & 4l^2(1+\frac{3}{4}\tau_1+\frac{19}{30}\tau_2+\frac{11}{20}\tau_3+\frac{17}{35}\tau_4) \end{bmatrix}$$

## References


Bishop, R. E. D. 1971 On the strength of large ships in heavy seas. *S. Afr. mech. Engng* **21**, 338.

Bishop, R. E. D., Eatock Taylor, R. & Jackson, K. L. 1973 On the structural dynamics of ship hulls in waves. *Trans. R. Inst. nav. Archit.* **115**, 257.

Bishop, R. E. D. & Eatock Taylor, R. 1973 On wave-induced stress in a ship executing symmetric motions. *Phil. Trans. R. Soc. Lond.* A **275**, 1.

Erdélyi, A. 1953 *Higher transcendental functions*, vol. 1. New York: McGraw-Hill.

Gallagher, R. H. & Lee, C. H. 1970 Matrix dynamic and instability analysis. *Int. J. num. Meth. Engng* **2**, 265.

Hylarides, S. 1971 Ship vibration analysis by finite element technique. Part 2. Vibration analysis. *Netherlands Ship Research Centre TNO* Report No. 153S.

Kendrick, S. 1970 The structural design of supertankers. *Trans. R. Inst. nav. Archit.* **112**, 391.

Kim, W. D. 1965 On the harmonic oscillations of a rigid body on a free surface. *J. Fluid Mech.* **21**, part 3, 427.

Kruppa, C. 1962 Beitrag zum Problem der hydrodynamischen Trägheitsgrossen bei elastischen Schiffsschwingungen. *Schiffstechnik* Bd. **9**, Heft 45.

Landweber, L. 1971 Natural frequencies of a body of revolution vibrating transversely in a fluid. *J. Ship Res.* **15**, 97.

Lewis, F. M. 1929 The inertia of water surrounding a vibrating ship. *Trans. Soc. nav. Archit. mar. Engrs* **37**, 1.

Lockwood Taylor, J. 1930 Some hydrodynamical inertia coefficients. *Phil. Mag.* **9** (series 7), 161.

Milne-Thomson, L. M. 1968 *Theoretical hydrodynamics*, 5th ed. London: MacMillan.

Salvadori, M. G. & Baron, M. L. 1961 *Numerical methods in engineering*, 2nd ed. London: Prentice-Hall.

Todd, F. H. 1961 *Ship hull vibration*. London: Edward Arnold.

Zienkiewicz, O. C. 1971 *The finite element method in engineering science*. London: McGraw-Hill.




PHILOSOPHICAL TRANSACTIONS OF THE ROYAL SOCIETY A MATHEMATICAL, PHYSICAL & ENGINEERING SCIENCES